Optical limiting and speckle of low power continuous wave laser beams using nonlinear scattering in photorefractive Zr: $LiNbO_3$ crystals

S. M. Kostritskii[a], O. G. Sevostyanov[b], M. Aillerie[c], and E. Kokanyan[d]

[a]RPC Optolink Ltd, Zelenograd, Russia; [b]Department of Physics, Institute of Basic Sciences, Kemerovo, Russia; [c]Centrale Supelec, LMOPS, Université de Lorraine, Metz, France; [d]Institute for Physical Research, Ashtarak, Armenia

ABSTRACT

The optical limiting caused by nonlinear scattering in the photore-fractive Zr-doped $LiNbO_3$ crystals was studied for lower-power laser beams with wavelengths of 514.5 and 532 nm. The measurements of speckle evolution indicate that the samples with $0.625 \leq [Zr] \leq 1.25$ mol% exhibit the very large gain factor for holographic amplifi-cation of noise gratings. Based on the direct measurements of the output power depending on the input one, we conclude that these samples behaved as hard optical limiters for the laser beams with a low incident power. Thus, these crystals find their potential applica-tion in the optical limiting devices.

1. Introduction

Over the past few years there has been a considerable interest in optical limiting (OL) of low power continuous wave (CW) laser beams using photorefractive (PR) materials [1,2]. Recently, iron-doped lithium niobate (Fe:$LiNbO_3$) has emerged as a very efficient optical limiter, producing changes in optical density (ΔOD) of up to 4 with l/e and switching speeds of a few milliseconds in a simple focal plane geometry [2]. The origin of the large ΔOD is an exceptionally high optical gain coefficient, which was reported to be as high as $100\,cm^{-1}$ [2].

The OL devices rely on one or more of the nonlinear optical mechanisms, which include excited saturation absorption (ESA), two-photon absorption (TPA), nonlinear refraction, nonlinear scattering (NLS), and PR self-defocusing [1–5]. NLS is a well-known phenomenon leading to OL in various media with nanoparticles [6,7]. As a result of the NLS, considerable portions of the energy will spread out into a wider spatial region and portion of light passing through an output aperture will be limited [1,7]. At the same time, a strong NLS was observed in the PR Zr-doped $LiNbO_3$ crystals, due to the very high magnitude of the optical gain coefficient Γ associated to the holographic amplification of a seed scattering [8,9]. According to all mentioned above findings [1,4–7], such a strong NLS is expected to provide good OL characteristics, demonstrating a linear transmittance below an OL threshold and clamps the output to

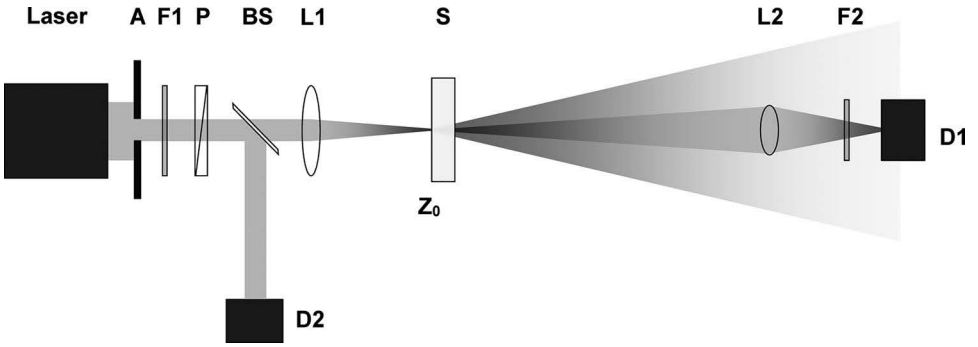

Figure 1. A schematic draw of the experimental set-up: L – laser, A – aperture, P – polarizer, S – sample, F1, F2 – neutral density filters, D1, D2 – detectors, BS – beam splitter, L1, L2 – lenses.

a practically constant above it, thus providing safety to sensors. In this article, we present our efforts and original results on application of the NLS in a series of PR Zr:$LiNbO_3$ crystals for OL.

2. Experimental

Based on the Czochralski technique, a set-up using a single platinum crucible with rf heating element in air atmosphere was used to grow a set of Zr-doped lithium niobate crystals [8,9]. In order to obtain single-domain crystals directly during the growth process, a dc electric current with a density of about 12 A/m^2 was passed through the crystal-melt system. The starting materials used for sintering the lithium niobate crystals of congruent composition were high purity Nb_2O_5 and $LiCO_3$ compounds from Johnson-Mattey and Merck. ZrO_2 was introduced into the melt with concentration equal to 0.625, 0.75, 0.875, 1.00, 1.25, 1.50, 2.00, and 2.50 mol%, respectively. The several nominally pure congruent $LiNbO_3$ samples were grown from a similarly prepared melt, but without addition of ZrO_2 compound. The latter samples were used to obtain the reference data in our study of Zr-doping effect. All samples were polished to the optical grade with surfaces perpendicular to the crystallographic axes.

The OL characteristics were studied using a set-up similar to the one used for our open-aperture (OA) Z-scan measurement [9], but at a fixed crystal position *z*. The transmitted and scattered beams were collected with a lens L2 in front of the detector D1 (Fig. 1). The incident laser intensity and its variations were measured with the reference detector D2. The lenses with the two different aperture sizes (20 and 70 mm) were used as L2 for our detailed studies of the speckle and OL, respectively. To perform the study of speckle dynamics, the small-aperture lens L2 and detector D1 were placed in far-field (L = 405 mm) behind a crystal, in contrast to OL study, in which the larger-aperture lens L2 was placed much closer (L = 162 mm) to the sample studied (Fig. 1).

Moreover, the speckle pattern was observed on a screen placed instead of the far-field lens L2 and detector D1. The intensity of the speckles in the transmitted beam was relatively weak. Above some threshold value of the input power, the intensity of the speckle pattern increased continuously with the input power.

Table 1. The values of NLS parameters for the moderately Zr-doped $LiNbO_3$ crystals. For rough estimation of these parameters at $P_{in} = 50$ mW, we use our previous Z-scan data on α_{nls} and Γ obtained at $P_{in} = 2$ mW ($\lambda = 514.5$ nm) [8, 9], and the data on dependence of Δn on P_{in} [9].

[Zr], mol %	0.625	0.88	1.0	1.5
α_{nls}, cm^{-1}, [8,9] (at $P_{in} = 2$ mW)	2.25	17.47	46.10	3.80
α_{nls}, cm^{-1} (at $P_{in} = 50$ mW)	12.5	68.3	112.4	16.7
Γ, cm^{-1}, [9] (at $P_{in} = 2$ mW)	15.1	15.9	10.3	3.9
Γ, cm^{-1} (at $P_{in} = 50$ mW)	56.5	79.2	67.4	18.5

The CW-radiation of an argon-ion laser "model 2550" (Spectra Physics, USA) at $\lambda = 514.5$ nm, or a DPSS laser "Mozart-5s" (Tekhnoscan-Lab, Russia) at $\lambda = 532$ nm was used in our experiments. The laser beam was focused with the 20-cm focal length L1 lens into the sample under study, as shown in Fig. 1. The input laser power was gradually varied within the range from 0.002 to 3.5 W that allowed comparing the speckle dynamics and OL in the Zr-doped and undoped $LiNbO_3$ crystals.

3. Results and discussion

Our previous OA Z-scan experiments with the moderately Zr-doped $LiNbO_3$ crystals ($0.625 \leq [Zr] \leq 1.5$ mol%) at low input powers ($0.5 \div 2$ mW) demonstrate the anomalously large NLS [8,9]. The significant magnitude of NLS can be seen as the wide-angle photoinduced light scattering (PILS) [9-11]. This NLS shows the pronounced dependence on the crystal position z relative to the reference z_0 given by the focal point of L1 [8,9], i.e. on a light intensity I, evidencing the PR origin of the NLS in $LiNbO_3$ crystals. The values of NLS coefficient α_{nls} [8] and gain factor Γ have been evaluated (Table 1). These values have been found to be dependent on a Zr concentration with the maximum values of Γ and α_{nls} at the intermediate doping level of $0.88 \leq [Zr] \leq 1.0$ mol%.

If a $LiNbO_3$ crystal with appropriate [Zr] ($0.625 \leq [Zr] \leq 1.5$ mol%) is placed in a fixed position z near focal point z_0 of the lens L1 [8] and it is illuminated by an extraordinary polarized CW-laser beam (Fig. 1), the power of output beam scattered by the crystal starts oscillating, if the input power P_{in} exceeds some threshold value P_{thr} (Fig. 2). It is related to the very strong NLS with the extremely large values of α_{nls} and Γ at $P_{in} \geq P_{thr}$ (Table 1). The estimation of Γ values was made by:

$$\Gamma = 4\pi\Delta n/(\lambda \cos\Theta_s) \quad (1)$$

where Δn is a photoinduced refractive index change, and Θ_s is a half-angle of the PILS cone inside a crystal [8,9,11].

The threshold power depends non-monotonously on both the doping concentration [Zr] and the position z of a sample in the set-up. This threshold power varies in the wide range: $20 \leq P_{thr} \leq 80$ mW. Typical plot of this self-pulsing phenomenon reported in Fig. 2 shows a noisy quasi-periodic time-dependence P_{out} in the moderately Zr-doped $LiNbO_3$. Both the amplitude and period of the output power oscillations depend on P_{in} and z (Figs. 2–4) [8]. The specific period of these oscillations is typically about a second. It is important to note, that in the strongly Zr-doped ($[Zr] \geq 2.0$ mol%) samples the

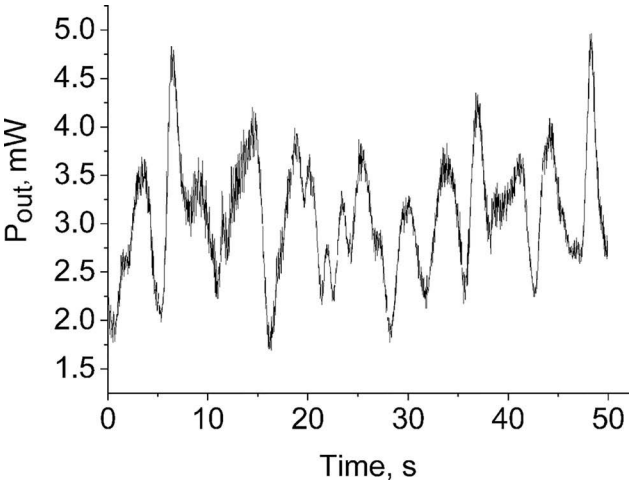

Figure 2. Temporal dependence of the self-pulsing phenomenon for forward-scattered laser beam measured in Zr-doped $LiNbO_3$ ([Zr] = 0.625 mol%) by the far-field detector D1 with the aid of a small-aperture lens (A = 20 mm) at the fixed crystal position $z = +23.8$ mm (i.e. crystal is shifted in right direction from focal point $z_0 = 0$ mm (Fig. 1). $P_{in} = 44$ mW and $\lambda = 514.5$ nm.

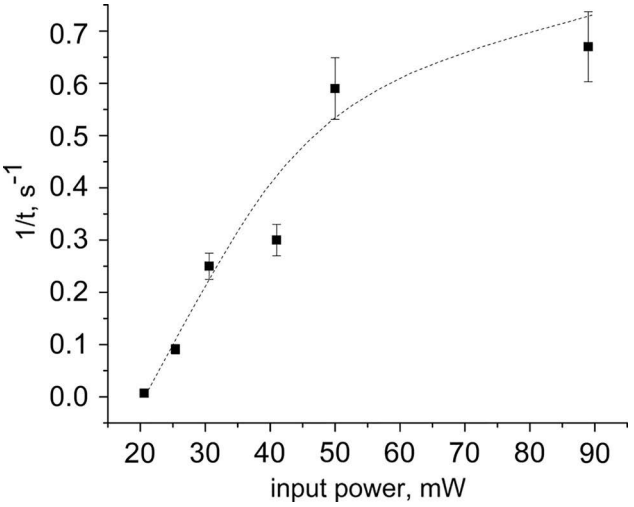

Figure 3. Self-pulsation frequency vs input power P_{in} measured at $z = +23.8$ mm and $\lambda = 514.5$ nm in the Zr-doped $LiNbO_3$ crystal with [Zr] = 0.625 mol%.

temporal evolution of NLS is different from what was observed in the moderately Zr-doped samples. Thus, the output power is static at steady-state (no any oscillations) in the samples having [Zr] $\geq$ 2.0 mol%, even at the largest P_{in} used by us.

The obvious light-induced speckle pattern is observed simultaneously with appearance of these oscillations. We observed that forward scattered patterns usually exhibited temporarily fluctuating tiny speckles. Morphology of such speckle patterns changed as a function of the position z between the focal point and the sample. After initial very fast conical defocusing, the pattern continued evolving in time into a picture of randomly moving speckles even in a steady-state, where no large scale structures could be

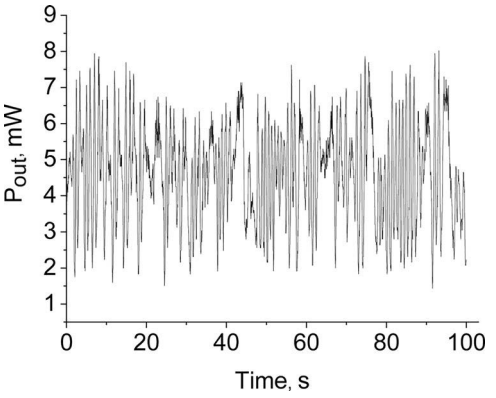

Figure 4. Temporal dependence of the self-pulsing phenomenon for forward-scattered laser beam measured in Zr-doped $LiNbO_3$ ([Zr] = 1.0 mol%) by the far-field detector D1 with the small aperture lens (A = 20 mm) at the fixed crystal position $z = 0$ mm. $P_{in} = 84$ mW and $\lambda = 514.5$ nm.

resolved. The maximum speckle-scattering angle was larger than that of the self-defocusing pattern regardless of the crystal position z [10].

According to recent finding [4–7], such a strong NLS should lead to good OL characteristics. In OL study with the set-up shown in Fig. 1, the laser beam is focused at a point in front of the crystal (i.e. z is ranged from -5 to $+5$ mm) by a lens L1 and the transmitted beam is collected with a large aperture lens L2 (aperture A = 70 mm) in front of the detector D1. Such a large aperture lens L2 has been applied for averaging (integration over main part of the moving speckles) of fluctuations caused by moving speckle, and for reduction of undesirable influence of the photorefractive self-focusing or self-defocusing effects [1,10]. The OL study is carried out by measurement of the output power P_{out} as a function of input power P_{in} (Fig. 5). If z ranged from -1 mm to $+1.5$ mm, then the marked fluctuations of the detected output power P_{out} would be observed, despite the averaging introduced with the aid of the large aperture lenses L2 (Fig. 6). Of course, the latter case is out of any practical interest of OL application. Depending on P_{in}, OL effect is much less pronounced or completely absent at $z < -5$ mm and $z > +5$ mm.

The related decrease in the transmittance can be understood, if we recall the geometric setup used for the OL experiments (Fig. 1). The apex angle in which transmitted probe light can be detected is given by the distance between the $LiNbO_3$ crystal and the lens L2, and the aperture size of this lens. In our setup, transmitted light can be collected by L2 within an apex angle of ±12.2°, whereas the NLS appears within a wider cone with $-16^\circ \geq \Theta_s \geq +16^\circ$ [11]; hence, some part of the scattered light propagates outside the detector D1 [8,9]. Note that aperture of the large-aperture lens L2 and the crystal-lens distance were specially adjusted to provide the necessary condition for appearance of OL caused by NLS [5,6]: a value of the apex angle for L2 should be smaller than the angle for the NLS cone. NLS is related to the photoinduced light scattering (PILS), which is explained by holographic amplification of the seed scattering due to the PR effect [8,9,11]. The PILS is observed in a multitude of PR materials: illumination with a focused laser beam leads to the build-up of scattered light into a wide apex angle around the directly transmitted laser beam. Hereby, an output power of the

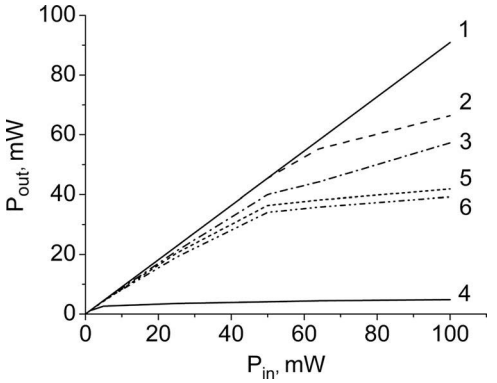

Figure 5. Optical limiting response measured at $z = +4$ mm in the undoped and Zr-doped $LiNbO_3$ crystals: (1) [Zr] = 0 (nominally pure congruent crystal) and [Zr] $\geq$ 2.0 mol%; (2) [Zr] = 1.5 mol%; (3) [Zr] = 0.625 mol%; (4) [Zr] = 1.0 mol%; (5) [Zr] = 1.25 mol%; (6) [Zr] = 0.88 mol%. P_{in} and P_{out} are input and output powers for a 514.5-nm laser beam.

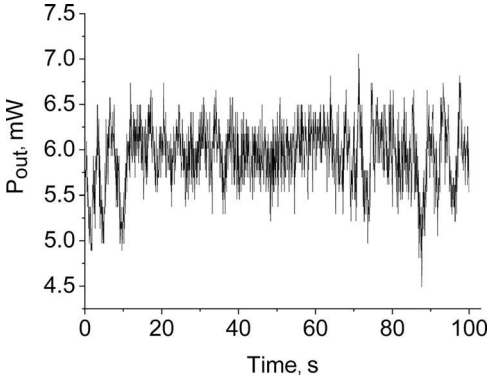

Figure 6. Temporal dependence of the output power for a laser beam transmitted through the Zr-doped $LiNbO_3$ ([Zr] = 1.0 mol%) and measured by the detector D1 with the large aperture lens L2 during OL experiment. This measurement made at the fixed crystal position $z = z_0 = 0$ mm at $P_{in} =$ 44 mW and $\lambda = 514.5$ nm.

transmitted beam is decreased, which can be as effective as 99% with respect to the incoming laser light power, i.e. the incoming pump beam can be nearly completely scattered in some particular cases [11].

The OL efficiency and OL threshold power have been estimated and found to be strongly dependent on Zr concentration with the extreme values at $0.88 \leq [Zr] \leq 1.25$ mol%. Note that OL threshold power is different from P_{thr} for self-pulsing experiments: OL threshold is lower than P_{thr}, depending on [Zr] and the largest difference is observed for the crystals with [Zr] = 1.0 mol% (Fig. 5, curve 4). Besides, OL threshold depends on z: threshold power increases with increasing z, but there is no proportionality between the threshold and z. The experimental input-output power curves reveal a hard limiting action above an OL threshold of P_{in} in crystals doped with $0.88 \leq [Zr] \leq 1.25$ mol% (Fig. 5, curves 4-6). The low OL threshold values in the range from 6 to 50 mW lead to a large dynamic range of the limiter. The hard limiting with these crystals is in contrast to the soft limiting observed in Zr-doped $LiNbO_3$ crystals

with the other Zr-doping levels ([Zr] = 0.625 and 1.5 mol%) (Fig. 5, curves 2 and 3). The experiments with the strongly Zr-doped crystals ([Zr] ≥ 2.0 mol%) show the small variations of P_{out} at high pump powers P_{in} (Fig. 5, curve 1), that is caused by the self-defocusing effect due to the light-induced change of the refractive index. The closed-aperture Z-scan study also shows that in the strongly Zr-doped crystals the refractive index nonlinearity is much smaller in comparison with the moderately Zr-doped and undoped $LiNbO_3$ crystals [12]. OL is observed also in the undoped LN, but at much higher powers. Thus, the OL threshold power is about 500 mW, that in $10 \div 83$ times higher than in the moderately Zr-doped $LiNbO_3$ crystals.

4. Conclusion

We present our efforts on application of the nonlinear light scattering (NLS) in Zr:$LiNbO_3$ crystals for optical limiting (OL). It has been established that the NLS in these crystals may be used in realizing an optical limiter. The experimental input-output power curves reveal a hard limiting action above a threshold of the input power in crystals doped with $0.88 \leq [Zr] \leq 1.25$ mol%. The hard limiting with these crystals is in contrast to the soft limiting observed in Zr:$LiNbO_3$ crystals with other Zr-doping levels. Besides, the original results on the detailed study of the NLS, including the speckle dynamics, and OL in the pure and Zr-doped $LiNbO_3$ crystals are reported.

Funding

This work was supported by Russian Foundation for Basic Research under RFBR Grant No 18-52-05012.

References

[1] J.-J. Liu, P. P. Banerjee, and Q. W. Song, Role of diffusive, photovoltaic, and thermal effects in beam fanning in $LiNbO_3$, *J. Opt. Soc. Am. B* **11** (9), 1688 (1994). DOI: 10.1364/JOSAB.11.001688.

[2] G. Cook *et al.*, Influence of the photovoltaic effect on optical limiting with lithium niobate, *Proc. SPIE* **4106**, 311 (2000). DOI: 10.1117/12.408518.

[3] L. W. Tutt, and T. F. Boggess, Review of optical limiting mechanisms and devices using organics, fullerenes, semiconductors and other materials, *Prog. Quantum Electron.* **17** (4), 299 (1993). DOI: 10.1016/0079-6727(93)90004-S.

[4] V. Joudrier *et al.*, Nonlinear light scattering in a two-component medium: Optical limiting application, *Appl. Phys. B* **67** (5), 627 (1998). DOI: 10.1557/PROC-479-279.

[5] V. Liberman *et al.*, Nonlinear bleaching, absorption, and scattering of 532-nm-irradiated plasmonic nanoparticles, *J. Appl. Phys.* **113** (5), 053107 (2013). DOI: 10.1063/1.4790798.

[6] N. Venkatram, R. S. S. Kumar, and D. N. Rao, Nonlinear absorption and scattering properties of cadmium sulphide nanocrystals with its application as a potential optical limiter, *J. Appl. Phys.* **100** (7), 074309 (2006). DOI: 10.1063/1.2354417.

[7] N. Venkatram, D. N. Rao, and M. A. Akundi, Nonlinear absorption, scattering and optical limiting studies of CdS nanoparticles, *Opt. Express.* **13** (3), 867 (2005). DOI: 10.1364/OPEX.13.000867.

[8] S. M. Kostritskii *et al.*, Nonlinear light scattering in photorefractive $LiNbO_3$ studied by Z-scan technique, *Appl. Phys. B* **125** (9), 160 (2019). DOI: 10.1007/s00340-019-7274-0.

[9] S. M. Kostritskii *et al.*, Parameters of nonlinear scattering evaluated by open-aperture Z-scan technique in photorefractive $LiNbO_3$ crystals, *Opt. Quant. Electron.* **52**, 92 (2020). DOI: 10.1007/s11082-020-2216-y.

[10] Q. W. Song, C. P. Zhang, and P. J. Talbot, Self-defocusing, self-focusing, and speckle in $LiNbO_3$ and $LiNbO_3$:Fe crystals, *Appl. Opt.* **32** (35), 7266 (1993). DOI: 10.1364/AO.32.007266.

[11] M. Goulkov, M. Imlau, and T. Woike, Photorefractive parameters of lithium niobate crystals from photoinduced light scattering, *Phys. Rev. B* **77** (23), 235110 (2008). DOI: 10.1103/PhysRevB.77.235110.

[12] S. M. Kostritskii, M. Aillerie, and E. Kokanyan. Investigation of nonlinear refraction and absorption in Mg- and Zr-doped $LiNbO_3$ with the aid of Z-scan techniques, *Proc. SPIE* **9065**, 906508 (2013). DOI: 10.1117/12.2051620.